

000 001 002 003 004 005 AURA: STRUCTURAL AND SEMANTIC CALIBRATION 006 FOR ROBUST FEDERATED GRAPH LEARNING 007 008 009

010 **Anonymous authors**
011 Paper under double-blind review
012
013
014
015
016
017
018
019
020
021
022
023
024
025
026
027
028
029
030

031 ABSTRACT

032 Training highly generalizable server model necessitates requires data from multiple
033 sources in Federated Graph Learning. However, noisy labels are increasingly
034 undermining federated system due to the propagation of erroneous information
035 between nodes. Compounding this issue, significant variations in data
036 distribution among clients make noise node detection more challenging. In our
037 work, we propose an effective structural and semantic calibration framework for
038 Robust Federated Graph Learning, **AURA**. We observe that spectral discrepancies
039 across different clients adversely affect noise detection. To address this,
040 we employs SVD for self-supervision, compelling the model to learn an intrinsic
041 and consistent structural representation of the data, thereby effectively attenuating
042 local high-frequency perturbations induced by noisy nodes. We introduce two metrics,
043 namely "Depth Influence" and "Breadth Influence". Based on these metrics, the framework
044 judiciously selects and aggregates the most consensual knowledge from the class prototypes
045 uploaded by each client. Concurrently, clients perform knowledge distillation by minimizing the KL
046 divergence between their local model's output distribution and that of the global model, which
047 markedly enhances the model's generalization performance and convergence stability
048 in heterogeneous data environments. **AURA** demonstrates remarkable robustness
049 across multiple datasets, for instance, achieving a 7.6% \uparrow F1-macro score
050 under a 20%-uniform noise on Cora. The code is available for anonymous access
051 at <https://anonymous.4open.science/r/AURA-F351/>.
052
053

1 INTRODUCTION

032 Federated Graph Learning (FGL), which combines the advantages of federated learning and graph
033 neural networks, is rapidly emerging as a significant research direction in distributed machine
034 learning. This approach enables multiple clients to collaboratively train a shared global model
035 while preserving the privacy of local graph data. It ensures effective privacy protection (13; 14) and
036 utilizes the neural message passing mechanism to learn representations from non-Euclidean data
037 structures. Such graph-structured data is prevalent in domains including biological networks (45),
038 urban transportation systems (44), and online social platforms (33).

039 Despite its potential, existing FGL research often relies on the idealized assumption of abundant and
040 accurate node labels. In practice, however, obtaining large-scale, high-quality labeled datasets is a
041 costly endeavor. Consequently, methods such as web scraping or utilizing user-generated content
042 for automatic label acquisition have become common. While these approaches reduce costs, they
043 inevitably introduce challenges related to label sparsity and noise.

044 It is well-established that neural networks are prone to overfitting noisy labels, which degrades their
045 generalization performance (28; 43). As a generalization of neural networks to the graph domain,
046 FGL models, as illustrated in Figure 1, exhibit similar performance degradation when trained
047 with noisy labels. A more severe issue arises from the inherent message-passing mechanism of
048 GNNs, which exacerbates the negative impact of label noise. Unlike independently and identically
049 distributed (i.i.d.) data, where a label error is isolated, an incorrect label on a single node can
050 propagate to its neighbors via graph edges. This process triggers cascading errors throughout the
051 multi-layer propagation of GNNs. This pollution propagation effect ultimately leads to a significant
052 degradation in the global model's performance, far exceeding the impact observed on i.i.d. data.

054
055
056
The complexity of this problem is further amplified within the federated learning framework, where
057
058
059
060
061
062
063
064
065
066
067
068
069
070
071
072
073
074
075
076
077
078
079
080
081
082
083
084
085
086
087
088
089
090
091
092
093
094
095
096
097
098
099
100
101
102
103
104
105
106
107
054
055
056
057
058
059
060
061
062
063
064
065
066
067
068
069
070
071
072
073
074
075
076
077
078
079
080
081
082
083
084
085
086
087
088
089
090
091
092
093
094
095
096
097
098
099
100
101
102
103
104
105
106
107
The complexity of this problem is further amplified within the federated learning framework, where
the unique graph topology of each client introduces significant heterogeneity.

From a structural perspective, node labels are not isolated attributes but are closely coupled with their local connectivity patterns. A clean label typically aligns with its neighborhood, manifesting as a smooth, low-frequency signal in the graph’s spectral domain. In contrast, a noisy label disrupts this local consistency, appearing as an abrupt, high-frequency anomaly. Significant structural differences among client graphs also lead to varied spectral compositions. For instance, in graphs with high homophily (e.g., social networks), noisy nodes generate more discernible high-frequency signals. Conversely, in graphs with complex connectivity patterns (e.g., biological molecular networks), these local anomalies can be easily obscured by the inherent structural noise. Consequently, noise detection methods effective in one spectral environment may fail in another. Thus, a key question arises: 1) *How can we design a framework that generalizes across heterogeneous client graphs by mining intrinsic structural patterns associated with label quality, to distinguish between clean and noisy nodes and mitigate performance degradation from client drift?*

From a semantic perspective, even if clients can learn representations that are more robust to local spectral and noise variations, the server still faces significant aggregation conflicts during the knowledge fusion stage. Due to spectral heterogeneity and the non-i.i.d. nature of the data, updates from different clients naturally carry different or even contradictory semantic directions. Consequently, the server receives multiple, potentially conflicting updates for the same conceptual class. If a simple averaging strategy like FedAvg is used, these differences are often blurred, leading to a global consensus that is either suboptimal or deviates from the correct direction. This naive aggregation approach not only fails to extract shared knowledge effectively but can also misguide the local models in subsequent rounds. Therefore, a more fundamental question is: 2) *How can we filter out local noise and drift while constructing a high-quality global knowledge base to guide all clients?*

To address the client drift issue arising from spectral heterogeneity, as identified in Problem I, we propose Structural-aware Frequency Alignment (SFA). This method utilizes Singular Value Decomposition (SVD) to perform a low-rank approximation of each client’s adjacency matrix. This process decomposes the original graph into two distinct views: a “structural backbone view” capturing core, low-frequency structural information, and a “redundant view” containing high-frequency and noise-related information. By enforcing representational consistency across these two views, our model performs dual denoising, simultaneously addressing inter-client heterogeneity and intra-client label noise. This approach effectively filters out high-frequency variations arising from structural differences among clients, thereby mitigating client drift. Moreover, this framework concurrently weakens the impact of local high-frequency disturbances caused by mislabeled nodes. The resulting node embeddings are highly robust to both noise and drift, providing a solid foundation for downstream tasks.

To address the semantic aggregation conflicts in Problem II, we propose Semantic-guided Consensus Distillation (SCD). The core of SCD is constructing a stable, high-quality global prototype graph to serve as a “semantic anchor” for alignment across all clients. On the client side, we first define depth influence and breadth influence, then select and aggregate local key information based on these metrics before uploading it to the global model. On the server side, a similarity-based selection mechanism aggregates the most consensual knowledge from client-uploaded category prototypes to build this global graph. Clients continue to employ relational knowledge distillation. By minimizing the Kullback-Leibler divergence between the similarity distributions of local and global model outputs with respect to the global prototypes, we compel the local model to emulate the global model’s understanding of the semantic relationships within the prototype graph. This approach elevates knowledge transfer from a hard, vector-level alignment to a soft, semantic-relational

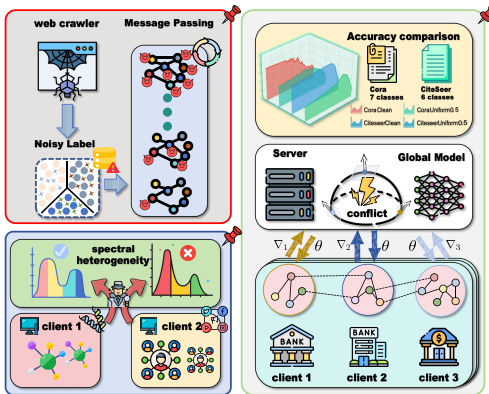


Figure 1: **Problem Illustration.** For current robust FGL scenarios: **I**) As illustrated in the top-right subplot, noisy labels have a severely detrimental effect on the server model’s performance, causing a performance drop of nearly 50%. **II**) The heterogeneity of data distributions across clients poses a significant challenge to the detection of noisy nodes.

From a semantic perspective, even if clients can learn representations that are more robust to local spectral and noise variations, the server still faces significant aggregation conflicts during the knowledge fusion stage. Due to spectral heterogeneity and the non-i.i.d. nature of the data, updates from different clients naturally carry different or even contradictory semantic directions. Consequently, the server receives multiple, potentially conflicting updates for the same conceptual class. If a simple averaging strategy like FedAvg is used, these differences are often blurred, leading to a global consensus that is either suboptimal or deviates from the correct direction. This naive aggregation approach not only fails to extract shared knowledge effectively but can also misguide the local models in subsequent rounds. Therefore, a more fundamental question is: 2) *How can we filter out local noise and drift while constructing a high-quality global knowledge base to guide all clients?*

To address the client drift issue arising from spectral heterogeneity, as identified in Problem I, we propose Structural-aware Frequency Alignment (SFA). This method utilizes Singular Value Decomposition (SVD) to perform a low-rank approximation of each client’s adjacency matrix. This process decomposes the original graph into two distinct views: a “structural backbone view” capturing core, low-frequency structural information, and a “redundant view” containing high-frequency and noise-related information. By enforcing representational consistency across these two views, our model performs dual denoising, simultaneously addressing inter-client heterogeneity and intra-client label noise. This approach effectively filters out high-frequency variations arising from structural differences among clients, thereby mitigating client drift. Moreover, this framework concurrently weakens the impact of local high-frequency disturbances caused by mislabeled nodes. The resulting node embeddings are highly robust to both noise and drift, providing a solid foundation for downstream tasks.

To address the semantic aggregation conflicts in Problem II, we propose Semantic-guided Consensus Distillation (SCD). The core of SCD is constructing a stable, high-quality global prototype graph to serve as a “semantic anchor” for alignment across all clients. On the client side, we first define depth influence and breadth influence, then select and aggregate local key information based on these metrics before uploading it to the global model. On the server side, a similarity-based selection mechanism aggregates the most consensual knowledge from client-uploaded category prototypes to build this global graph. Clients continue to employ relational knowledge distillation. By minimizing the Kullback-Leibler divergence between the similarity distributions of local and global model outputs with respect to the global prototypes, we compel the local model to emulate the global model’s understanding of the semantic relationships within the prototype graph. This approach elevates knowledge transfer from a hard, vector-level alignment to a soft, semantic-relational

108 one, significantly enhancing generalization and stability. This framework accurately decouples label
 109 noise and interference from spectral heterogeneity while ensuring excellent performance. We name
 110 the combination of these two strategies **AURA**, the Structural and Semantic Calibration framework
 111 for Robust Federated Graph Learning. Our main contributions are summarized as follows:
 112

- 113 • We address the challenging problem of defending against noisy labels in FGL. We identify the key
 114 challenges as learning representations robust to the dual interference of intra-client label noise and
 115 inter-client spectral heterogeneity, and constructing a high-quality global knowledge base while
 116 mitigating the effects of local noise and client drift.
- 117 • We propose **AURA**, a novel framework that combats noisy labels in FGL via a dual strategy of
 118 Representation Purification and Knowledge Alignment.
- 119 • We conduct extensive experiments on five mainstream datasets under various noise types and
 120 ratios. The results demonstrate that our approach significantly outperforms existing state-of-the-
 121 art FGL methods. For instance, under the 20% uniform noise setting on the Cora dataset, our
 122 method outperforms the second-best method by a significant margin of 7.6% in F1-macro score.

123 2 PRELIMINARIES

124 **Notations.** We follow the general paradigm of federated graph learning, K participants (indexed by
 125 k) collaboratively train a shared global model using their private graph data. Participant k holds a
 126 graph $\mathcal{G}_k = (\mathcal{V}_k, \mathcal{A}_k, \mathcal{X}_k)$, where $\mathcal{V}_k = \{v_i\}_{i=1}^{N_k}$ is the node set containing $|\mathcal{V}_k| = N_k$ nodes, $\mathcal{A}_k \in$
 127 $\{0, 1\}^{N_k \times N_k}$ is the adjacency matrix with $A_{ij} = 1$ if there is an edge between nodes v_i and v_j (and
 128 0 otherwise). Similarly, \mathcal{X}_k represents node features, and \mathcal{Y}_k represents the corresponding label set.

129 **Problem Formulation.** To evaluate the robustness of our method, we take the semi-supervised
 130 node classification on the graph as the pretext task which can be defined as follows. We split all
 131 the nodes \mathcal{V} into three sets \mathcal{V}^{train} , \mathcal{V}^{val} and \mathcal{V}^{test} for training, validation, and testing respectively.
 132 After label contamination, $\tilde{\mathcal{Y}}$ is divided into the ground truth labels \mathcal{Y} and the corrupted labels $\tilde{\mathcal{Y}}$.
 133 When learning representations in noisy label scenarios, clean nodes and noisy nodes in \mathcal{V}^{train} are
 134 available. Besides, given \mathcal{X}_k and \mathcal{A}_k , the goal of node classification is to train a classifier $Enc_{\theta_k} : (135$
 $(\mathcal{X}_k, \mathcal{A}_k) \rightarrow \hat{\mathcal{Y}}_k$, where the model parameters are optimized by minimizing the following objective:
 136

$$137 \min_{\theta_k} \mathcal{L}(Enc_{\theta_k}(\mathcal{X}_k, \mathcal{A}_k), \mathcal{Y}_k), \quad (1)$$

138 where \mathcal{L} is a loss function that quantifies the discrepancy between predictions and ground-truth
 139 labels. In accordance with the principle of Empirical Risk Minimization (ERM), the well-trained
 140 classifier Enc_{θ_k} is capable of generalizing well to unseen nodes in \mathcal{V}^{test} .
 141

142 **Uniform noise (34):** This noise model assumes that the true label has a probability $\in (0, 1)$ of being
 143 uniformly flipped to any of the other classes with equal probability. Formally, for all $j \neq i$,

$$144 p(y_m^N = j \mid y_m^L = i) = \frac{\epsilon}{d-1}. \quad (2)$$

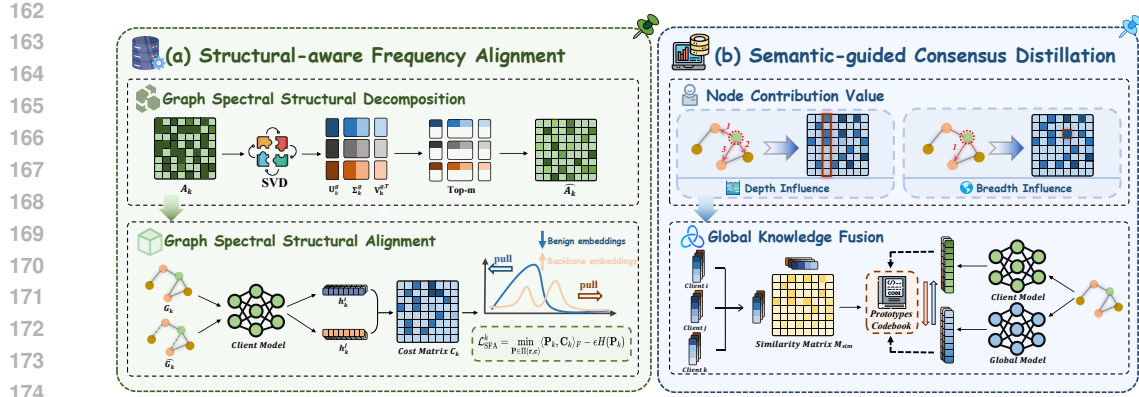
145 **Pair noise (41):** This noise model assumes that the true label can only be flipped to a specific paired
 146 class with a fixed probability ϵ , while remaining unchanged with probability $1 - \epsilon$.
 147

148 The optimization objective is to learn a generalizable global model through the federated learning
 149 process that performs well under noisy conditions while maintaining strong robustness.
 150

151 3 METHODOLOGY

152 3.1 STRUCTURAL-AWARE FREQUENCY ALIGNMENT (SFA)

153 **Motivation.** Significant structural differences among client graphs lead to varied spectral compo-
 154 sitions. Consequently, a noise detection method effective in one spectral environment may prove
 155 ineffective in another. To design a noise filtering framework that is insensitive to these spectral vari-
 156 ations, we propose Structural-aware Frequency Alignment (SFA). This method leverages Singular
 157 Value Decomposition (SVD) to perform a low-rank approximation of each client’s adjacency matrix,
 158 simultaneously addressing both inter-client heterogeneity and intra-client label noise. **Graph Spec-
 159 tral Structural Decomposition.** To create the structural backbone view, we perform a low-rank
 160

Figure 2: **Architecture illustration** of AURA. Best viewed in color and zoom in for details.

approximation on each client’s adjacency matrix \mathbf{A}_k . First, we apply Singular Value Decomposition (SVD) to decompose \mathbf{A}_k into its constituent structural components:

$$\mathbf{A}_k = \mathbf{U}_k \Sigma_k \mathbf{V}_k^T, \quad (3)$$

where \mathbf{U}_k and \mathbf{V}_k^T are orthogonal matrices of left and right singular vectors, and Σ_k is a diagonal matrix of singular values. The singular values in Σ_k represent the importance of their corresponding structural patterns. In particular, the largest singular values in Σ_k and their corresponding vectors capture the most dominant, low-frequency structural patterns.

Multiple articles (8; 6) demonstrate that these core structural patterns are more critical for learning robust node representations than high-frequency details or noise. We posit that these patterns form the graph’s structural backbone and are more critical for learning robust representations. Conversely, the smaller singular values correspond to high-frequency details, which can include both client-specific structural heterogeneity and noise from sources like incorrect labels.

Therefore, we construct the low-frequency backbone view by retaining only the top-m singular values and their corresponding vectors, effectively capturing the essential structural information. Let $\mathbf{U}_k^{[1:m]}$, $\Sigma_k^{[1:m]}$ and $\mathbf{V}_k^{[1:m]}$ be the truncated matrices corresponding to the top-m singular values. The reconstructed, low-frequency adjacency matrix, $\hat{\mathbf{A}}_k$, is then reconstructed as:

$$\hat{\mathbf{A}}_k = \mathbf{U}_k^{[1:m]} \Sigma_k^{[1:m]} \mathbf{V}_k^{[1:m]T}. \quad (4)$$

This matrix $\hat{\mathbf{A}}_k$ serves as a low-pass filtered representation of the original graph structure, preserving its most salient connectivity patterns while discarding finer, potentially disruptive information.

Graph Spectral Structural Alignment. This decomposition process yields two structural views for each client k : the original graph, \mathbf{G}_k , defined by \mathbf{A}_k , and the structural backbone view, $\hat{\mathbf{G}}_k$, defined by $\hat{\mathbf{A}}_k$. We then pass both views through our GNN encoder to obtain two sets of node representations. Correspondingly, let \mathbf{h}_k denote the embeddings from the original graph \mathbf{G}_k , and $\hat{\mathbf{h}}_k$ denote the embeddings from the reconstructed graph $\hat{\mathbf{G}}_k$.

We treat these two embeddings as empirical distributions over the embedding manifold and align their global geometry using Optimal Transport (OT). Traditional alignment methods fail to capture cross-dimensional similarities, leading to the underutilization of dimensional information. To address this issue, we propose a Sinkhorn distance-based embeddings alignment method, which deploys the discrete Sinkhorn distance to comprehensively measure the distributional differences between both embeddings. We first define a ground cost matrix $\mathbf{C} \in \mathbb{R}^{N_k \times N_k}$, where \mathbf{C}_{ij} is the cost of matching node v_i from the original view to node v_j from the backbone view. Specifically, in our implementation, a natural choice is the cosine distance:

$$\mathbf{C}_k^{ij} = 1 - \text{sim}(\mathbf{h}_k^i, \hat{\mathbf{h}}_k^j). \quad (5)$$

The SFA loss is then formulated as the Sinkhorn distance, a computationally efficient and differentiable approximation of the OT distance. It seeks a transport plan $\mathbf{P} \in \mathbb{R}^{N_k \times N_k}$ that minimizes the

216 total transportation cost while satisfying marginal constraints. The loss is defined as:
 217

$$\mathcal{L}_{\text{SFA}}^k = \text{Sinkhorn}(\mathbf{H}_k, \hat{\mathbf{H}}_k) = \min_{\mathbf{P} \in \Pi(\mathbf{r}, \mathbf{c})} \langle \mathbf{P}_k, \mathbf{C}_k \rangle_F - \epsilon H(\mathbf{P}_k) \quad (6)$$

220 where $\langle \cdot, \cdot \rangle_F$ is the Frobenius dot product, which calculates the total transportation cost. It is
 221 computed by summing the element-wise products of the transport plan \mathbf{P} and the cost matrix
 222 \mathbf{C}_k . Specifically, $\langle \mathbf{P}_k, \mathbf{C}_k \rangle_F = \sum_{i,j} \mathbf{P}_{ij} \mathbf{C}_{ij}$. $\Pi(\mathbf{r}, \mathbf{c})$ is the set of joint probability matrices with
 223 uniform marginals \mathbf{r} and \mathbf{c} , $H(\mathbf{P}) = -\sum_{i,j} \mathbf{P}_{ij} \log \mathbf{P}_{ij}$ is the Shannon entropy of the transport
 224 plan, and $\epsilon > 0$ is the entropic regularization parameter.
 225

226 3.2 SEMANTIC-GUIDED CONSENSUS DISTILLATION (SCD) 227

228 **Motivation.** Even when clients can learn representations resilient to local spectral and noise variations,
 229 the server still confronts significant aggregation conflicts. These conflicts arise when updates
 230 for the same conceptual class from different clients are mutually contradictory. To mitigate this
 231 issue, we propose Semantic-guided Consensus Distillation (SCD), which constructs a stable, high-
 232 quality global prototype graph to serve as a "semantic anchor" for alignment across all clients.
 233

234 **Node Contribution Value.** To effectively filter core nodes within a knowledge graph and optimize
 235 the client-side knowledge extraction process, we propose a contribution assessment method based on
 236 the semantic influence of nodes. This method comprehensively considers both the Breadth Influence
 237 and Depth Influence of a node to more thoroughly characterize its importance within the knowledge
 238 network. We define the contribution of a node from the following two dimensions:
 239

240 **Depth Influence:** This metric aims to measure the core capability of a node to be strongly
 241 influenced by its local context. It is defined as the maximum influence value exerted on the
 242 node by any of its adjacent nodes, reflecting the strongest associative relationship it possesses.
 243 A node with high Depth Influence signifies that it has an exceptionally close semantic
 244 connection with at least one or more other nodes.
 245

246 **Breadth Influence:** This metric is designed to measure the centrality of a node as an
 247 information convergence point within the network. It is defined as the cumulative sum
 248 of influence exerted by all other nodes in the network onto the target node, reflecting the
 249 extensiveness of the influence it receives. A node with high Breadth Influence typically serves
 250 as an intersection point for multiple knowledge paths.
 251

252 The calculation process primarily involves the construction of an influence matrix, the quantification
 253 of breadth and depth influences, and the final fusion to compute the contribution score. The influence
 254 matrix is calculated based on a random walk model, which can capture the indirect influence
 255 transmitted between nodes through multi-step paths. This model simulates the flow of information
 256 along the graph's edges. First, we construct the random walk transition matrix P of the graph:
 257

$$P = D^{-1} A \quad (7)$$

258 where A is the adjacency matrix of the knowledge graph, and D is the degree matrix, a diagonal
 259 matrix whose elements are the degrees of the corresponding nodes.
 260

261 Building on this, we introduce a mechanism similar to Personalized PageRank to compute a global
 262 influence matrix M . This matrix not only considers direct connections but also incorporates multi-
 263 step reachability relationships weighted by a decay factor:
 264

$$M = \alpha (I - (1 - \alpha)P)^{-1} \quad (8)$$

265 where I is the identity matrix, and $\alpha \in (0, 1)$ is a smoothing factor used to balance the probabilities
 266 between the random walk and a global jump. An element $M_{i,j}$ in matrix M represents the influence
 267 from node j on node i , quantifying how much node j contributes to the representation learning of
 268 node i through all possible paths in the graph. For any given node i , $Score_i^b$ is calculated as follows:
 269

$$Score_i^b = \frac{\sum_{j \in \mathcal{V}^{\text{train}}} M_{j,i}}{Z} \quad (9)$$

270 where \mathcal{V}_L represents the set of all nodes in the graph, and the numerator sums the influence from all
 271 nodes on node i . Z is a normalization factor. The Depth Influence, $Score_i^d$, is calculated as:
 272

$$273 \quad Score_i^d = \max_{j \in \mathcal{N}(i)} (M_{j,i} \cdot \tau_j) \quad (10)$$

274

275 where $\mathcal{N}(i)$ is the set of neighboring nodes of node i , and τ_j is an optional weight or type coefficient
 276 for node j , used to adjust the importance of different nodes. This formula captures the strongest
 277 determinative signal influencing node i from its immediate neighborhood. Finally, we perform a
 278 linear weighted sum of the node's breadth and depth influences to obtain its final contribution score:
 279

$$280 \quad Score_i = Score_i^b + \beta \cdot Score_i^d \quad (11)$$

281

282 where β is a hyperparameter used to adjust the weight of the Depth Influence in the total contribu-
 283 tion score. By calculating $Score_i$ for each node, we can quantify its importance in the graph and
 subsequently set a threshold to filter out nodes with low influence.

284 **Global Knowledge Fusion.** We posit that the nodes with the highest scores constitute the Semantic
 285 Core of each client's training set, serving as the most distinct and unambiguous representatives of
 286 their respective classes. Therefore, we select only the nodes ranking in the top-1/3 based on their
 287 scores from each client \mathcal{V}_k (denoted as \mathcal{V}_k^*) to generate local prototypes. For each class c , the local
 288 prototype \mathbf{p}_k^c for client k is computed as follows:
 289

$$290 \quad \mathbf{p}_k^c = \frac{1}{|\mathcal{V}_k^{*c}|} \sum_{u \in \mathcal{V}_k^{*c}} \mathbf{h}_u \quad (12)$$

291

292 where \mathcal{V}_k^{*c} is the set of semantic core nodes belonging to class c on client k , and \mathbf{h}_u is the embedding
 293 of node u . Upon completion of the local computations, each client uploads its generated prototypes
 294 and the corresponding sample counts per class to the central server. The server's objective is not to
 295 naively average them, but rather to identify and fuse the prototypes that exhibit the highest consensus
 296 and are most representative of the global distribution, in order to synthesize Global Anchors.
 297

298 The server first assesses the mutual consistency among the local prototypes within a randomly se-
 299 lected subset of clients \mathcal{N}_t^c (controlled by a participation rate α). For each class c , the server con-
 300 structs a prototype similarity matrix M_{sim}^c , where each element is defined by cosine similarity:
 301

$$302 \quad M_{sim}^{ij} = \text{sim}(\mathbf{p}_i^c, \mathbf{p}_j^c) = \frac{(\mathbf{p}_i^c)^T \mathbf{p}_j^c}{\|\mathbf{p}_i^c\| \|\mathbf{p}_j^c\|}, \quad \forall i, j \in \mathcal{N}_t^c \quad (13)$$

303

304 Based on this similarity matrix, the server computes a Global Cohesion Score S_i^c for each local
 305 prototype. This score quantifies the degree of agreement between a given local prototype and all
 306 others. A high-scoring prototype signifies that it has garnered consensus from a majority of other
 307 clients, making it more likely to reside at the center of the global class distribution.
 308

$$309 \quad S_i^c = \sum_{j \in \mathcal{N}_t^c, j \neq i} M_{sim}^{ij} \quad (14)$$

310

311 Finally, for each class c , the server refrains from blindly averaging all prototypes. Instead, it selects
 312 only the top-K local prototypes with the highest Global Cohesion Scores for aggregation, thereby
 313 synthesizing the final Global Anchor prototype \mathbf{P}_g^c .
 314

315 **Local Knowledge Alignment.** To guide local training, we implement a federated knowledge
 316 distillation scheme once the global model and the anchor prototype graph (\mathbf{P}_g^c) are disseminated
 317 to the clients. In this framework, the received global model acts as a "teacher," providing semantic
 318 guidance, while the local model acts as a "student." The knowledge transfer focuses on relational
 319 understanding rather than direct feature mimicry. Specifically, we compel the student model to
 320 replicate the teacher's perception of how a node's features relate to the global prototypes.
 321

322 This is achieved by aligning their respective similarity distributions. For each node u , we generate
 323 a target distribution by first obtaining its feature representation \mathbf{h}_u^g from the frozen teacher model.
 324 We then compute the cosine similarities between \mathbf{h}_u^g and all prototypes in \mathbf{P}_g using a function φ ,
 325 and normalize these scores into a probability distribution via the softmax function σ . The student

Table 1: Performance comparison to state-of-the-art methods when poisoning 50% of the full set. We report accuracy (%) and F1-macro (%) (with red/green markers indicating regression/improvement over FedAvg). The best and second-best results are highlighted with **Blue** and underline, respectively. Additional experimental results on more settings can be found in Appendix G.

Dataset		CORA (Acc \uparrow)			CITESEET (Acc \uparrow)			PUBMED (Acc \uparrow)		
	Noise Type	Normal	Uniform	Pair	Normal	Uniform	Pair	Normal	Uniform	Pair
Normal	FedAvg [ASTAT17]	74.50 \pm 0.00	48.17 \pm 0.00	37.20 \pm 0.00	64.15 \pm 0.00	32.59 \pm 0.00	34.22 \pm 0.00	84.16 \pm 0.00	78.31 \pm 0.00	58.53 \pm 0.00
	FedProx [MLSys20]	75.32 \pm 0.82	48.26 \pm 0.09	33.73 \pm 0.47	65.19 \pm 0.04	33.04 \pm 0.45	34.81 \pm 0.59	84.24 \pm 0.08	78.47 \pm 0.16	58.32 \pm 0.21
	FedDC [CVPR22]	80.90 \pm 0.40	46.25 \pm 0.92	38.85 \pm 0.65	67.85 \pm 0.70	38.22 \pm 0.63	37.04 \pm 0.82	82.91 \pm 0.35	40.18 \pm 0.13	50.73 \pm 0.78
	FedDyn [ICLR21]	79.98 \pm 0.58	44.42 \pm 0.75	38.48 \pm 0.20	69.04 \pm 0.89	34.96 \pm 0.37	35.11 \pm 0.89	81.83 \pm 0.23	74.77 \pm 0.54	51.90 \pm 0.63
	Scaffold [ICML20]	81.90 \pm 0.74	56.12 \pm 0.75	43.42 \pm 0.22	70.22 \pm 0.07	40.44 \pm 0.75	37.93 \pm 0.71	75.25 \pm 0.91	64.02 \pm 14.29	52.56 \pm 0.97
	FedGTA [VLDB24]	72.21 \pm 0.29	51.83 \pm 0.64	36.56 \pm 0.64	65.33 \pm 0.18	37.33 \pm 0.47	36.15 \pm 0.93	82.41 \pm 0.75	79.20 \pm 0.88	57.24 \pm 0.29
	FedTAD [IJCAI24]	64.90 \pm 0.60	46.89 \pm 0.28	38.76 \pm 0.56	64.30 \pm 0.50	32.44 \pm 0.15	34.81 \pm 0.59	84.36 \pm 0.20	77.23 \pm 0.01	61.51 \pm 0.29
Robust	FGSSL [IJCAI23]	68.74 \pm 0.16	57.40 \pm 0.23	34.28 \pm 0.92	70.07 \pm 0.92	48.59 \pm 1.00	39.41 \pm 0.19	67.03 \pm 17.13	66.40 \pm 11.91	56.43 \pm 0.20
	Coteaching [NeurIPS18]	72.03 \pm 0.24	45.43 \pm 0.74	39.03 \pm 1.83	64.30 \pm 0.15	41.48 \pm 0.89	35.85 \pm 0.63	84.26 \pm 0.10	76.85 \pm 0.46	60.02 \pm 0.49
	FedNoRo [IJCAI23]	74.50 \pm 0.00	42.34 \pm 0.58	34.96 \pm 0.24	67.76 \pm 0.31	30.37 \pm 0.22	32.99 \pm 0.23	84.16 \pm 0.00	77.03 \pm 0.28	44.97 \pm 13.56
	FedNed [AAAI24]	69.84 \pm 0.66	35.37 \pm 1.20	34.40 \pm 0.74	57.78 \pm 0.67	29.63 \pm 0.96	31.11 \pm 0.11	84.56 \pm 0.40	62.32 \pm 15.95	53.09 \pm 0.44
	FedCorr [CVPR22]	75.14 \pm 0.64	52.01 \pm 0.84	36.20 \pm 0.00	38.96 \pm 0.59	26.07 \pm 0.52	29.04 \pm 0.18	85.93 \pm 0.77	68.93 \pm 0.39	48.91 \pm 09.62
	CRGNN [NN24]	72.30 \pm 0.20	49.36 \pm 0.19	38.03 \pm 0.83	69.33 \pm 0.18	33.78 \pm 0.19	38.81 \pm 0.59	84.08 \pm 0.08	40.11 \pm 38.20	59.72 \pm 0.19
	RTGNN [WWW23]	71.46 \pm 0.04	46.62 \pm 0.55	35.28 \pm 0.83	67.85 \pm 0.70	51.11 \pm 18.52	37.19 \pm 0.97	60.10 \pm 0.46	68.09 \pm 0.22	47.01 \pm 11.52
Normal	CLNode [WSDM23]	69.65 \pm 0.85	36.56 \pm 1.11	35.47 \pm 0.73	59.11 \pm 0.05	28.59 \pm 0.04	30.37 \pm 0.85	84.99 \pm 0.83	79.93 \pm 0.32	53.39 \pm 05.14
	AURA	85.22 \pm 10.72	61.64 \pm 13.47	46.27 \pm 09.07	77.23 \pm 13.08	52.38 \pm 19.79	46.28 \pm 12.06	85.95 \pm 01.79	80.44 \pm 02.13	57.53 \pm 01.00
	Whole Dataset	48.04 \pm 0.9			36.94 \pm 0.3			69.49 \pm 0.5		
	Dataset	COAUTHOR-PHYSICS (F1-macro \uparrow)			MINESWEEPER (F1-macro \uparrow)			COAUTHOR-CS (F1-macro \uparrow)		
	Noise Type	Normal	Uniform	Pair	Normal	Uniform	Pair	Normal	Uniform	Pair
	FedAvg [ASTAT17]	24.18 \pm 0.00	13.76 \pm 0.00	27.10 \pm 0.00	53.51 \pm 0.00	33.40 \pm 0.00	19.38 \pm 0.00	02.47 \pm 0.00	02.47 \pm 0.00	02.47 \pm 0.00
	FedProx [MLSys20]	23.22 \pm 0.96	17.50 \pm 03.74	25.55 \pm 01.55	53.54 \pm 0.03	33.30 \pm 0.10	19.35 \pm 0.03	02.76 \pm 00.29	02.45 \pm 00.02	03.76 \pm 01.29
Robust	FedDC [CVPR22]	13.55 \pm 10.63	13.46 \pm 0.30	14.45 \pm 12.65	53.59 \pm 0.08	35.51 \pm 0.11	16.60 \pm 0.78	03.22 \pm 00.75	01.90 \pm 0.57	03.43 \pm 0.96
	FedDyn [ICLR21]	15.78 \pm 08.40	15.51 \pm 01.75	27.32 \pm 00.22	51.22 \pm 02.29	37.70 \pm 04.30	16.23 \pm 03.15	06.38 \pm 03.91	02.47 \pm 00.00	02.47 \pm 00.00
	Scaffold [ICML20]	42.61 \pm 18.43	13.46 \pm 0.30	05.13 \pm 21.97	44.25 \pm 09.26	41.46 \pm 08.06	18.99 \pm 08.11	04.46 \pm 00.01	02.42 \pm 00.05	02.76 \pm 00.29
	FedGTA [VLDB24]	13.72 \pm 10.46	17.48 \pm 03.72	16.24 \pm 10.86	53.58 \pm 00.07	33.19 \pm 04.21	21.43 \pm 05.67	01.35 \pm 01.12	03.17 \pm 00.70	02.59 \pm 00.92
	FedTAD [IJCAI24]	22.13 \pm 02.05	14.52 \pm 01.66	08.80 \pm 18.30	54.11 \pm 01.60	32.35 \pm 01.05	20.12 \pm 06.98	02.47 \pm 00.00	02.56 \pm 00.09	06.68 \pm 04.21
	FGSSL [IJCAI23]	28.13 \pm 03.95	13.58 \pm 01.18	05.06 \pm 22.04	44.46 \pm 09.05	43.50 \pm 10.10	16.23 \pm 10.87	02.83 \pm 06.36	02.89 \pm 00.42	00.31 \pm 02.16
	Whole Dataset	13.46 \pm 10.72	14.12 \pm 00.36	34.85 \pm 07.75	44.25 \pm 09.26	36.77 \pm 03.37	17.12 \pm 09.98	08.00 \pm 05.53	07.20 \pm 04.73	04.36 \pm 01.89
Normal	Coteaching [NeurIPS18]	22.46 \pm 01.72	13.96 \pm 00.20	27.10 \pm 00.00	53.54 \pm 00.03	33.40 \pm 00.00	17.87 \pm 09.23	02.49 \pm 00.02	03.01 \pm 00.54	02.49 \pm 00.02
	FedNoRo [IJCAI23]	35.94 \pm 11.76	13.79 \pm 09.40	22.88 \pm 04.22	51.97 \pm 01.54	38.67 \pm 05.27	26.58 \pm 07.20	11.85 \pm 09.38	06.80 \pm 04.33	05.33 \pm 02.16
	FedNed [AAAI24]	27.93 \pm 03.75	21.47 \pm 07.71	29.42 \pm 02.32	44.14 \pm 09.37	18.40 \pm 15.00	16.12 \pm 10.98	01.34 \pm 01.13	02.47 \pm 00.00	02.62 \pm 00.16
	FedCorr [CVPR22]	35.12 \pm 10.94	26.97 \pm 13.21	35.83 \pm 08.73	46.78 \pm 06.73	17.09 \pm 16.31	16.78 \pm 02.60	13.08 \pm 10.61	07.31 \pm 04.84	11.09 \pm 08.62
	CRGNN [NN24]	33.17 \pm 08.99	13.78 \pm 00.02	05.06 \pm 22.04	43.93 \pm 09.58	48.27 \pm 14.87	31.20 \pm 11.82	02.47 \pm 00.00	02.52 \pm 00.05	02.47 \pm 00.00
	RTGNN [WWW23]	40.78 \pm 16.60	23.25 \pm 09.49	22.80 \pm 04.30	53.93 \pm 04.02	36.59 \pm 03.19	29.94 \pm 10.58	06.83 \pm 03.46	06.79 \pm 04.32	05.68 \pm 03.21
	CLNode [WSDM23]	57.99 \pm 33.81	68.87 \pm 55.11	54.13 \pm 27.03	55.29 \pm 01.78	49.68 \pm 15.88	47.12 \pm 27.74	21.80 \pm 19.33	22.31 \pm 19.84	15.11 \pm 12.64
Whole Dataset		20.36 \pm 0.6			35.58 \pm 0.3			05.10 \pm 0.4		

model is then trained to minimize the Kullback-Leibler (KL) divergence between its own output distribution (derived from its feature h_u^i) and the teacher's target distribution. This objective is formalized as our Federated Knowledge Distillation loss:

$$\mathcal{L}_{\text{FKD}} = \frac{1}{|\mathcal{V}_i|} \sum_{u \in \mathcal{V}_i} \text{KL} \left(\sigma \left(\varphi(\mathbf{h}_u^i, \mathbf{P}_g) \right), \sigma \left(\varphi(\mathbf{h}_u^g, \mathbf{P}_g) \right) \right), \quad (15)$$

where KL divergence penalizes deviations in the student's relational reasoning from the teacher's. Furthermore, we provide the overall workflow of our framework in [Appendix D](#).

4 EXPERIMENT

In this section, we conduct extensive experiments to answer the following research questions: **(RQ1)** How does **AURA** perform compared to existing normal/ robust federated graph learning frameworks? **(RQ2)** What is the impact of each component of **AURA** on the overall performance? **(RQ3)** How sensitive is **AURA** to its key components and parameters?

4.1 EXPERIMENTAL SETUP

Datasets and Benchmarks. Adhering to (47), we evaluate the efficacy and robustness in five scenarios with different characteristics, including Cora (25), CiteSeer (9), PubMed (3), Physics (31), CS (32), and Minesweeper (2). Following (47), we adopt a 20%/20%/40% train/validation/test random split for the dataset. These datasets represent a wide range of domains and are commonly used in graph-based machine learning tasks. Detailed datasets information is provided in Appendix C.1.

Comparison Method. We compare AURA with several state-of-the-art methods in normal FGL and robust FGL: (1) **FedAvg** [ASTAT17] (26), (2) **FedProx** [MLSys20] (18), (3) **FedDC** [CVPR22] (7), (4) **FedDyn** [ICLR 21] (1), (5) **Scaffold** [ICML 20] (16), (6) **FedGTA** [VLDB24] (21), (7) **FedTAD** [IJCAI24] (47), (8) **FGSSL** [IJCAI23] (12), (9) **textbf{Coteaching}** [NeurIPS18] (10), (10) **FedNoRo** [IJCAI23] (39), (11) **FedNed** [AAAI24] (23), (12) **FedCorr** [CVPR22] (40); three Robust GraphLearning methods: (13) **CRGNN** [NN24] (20), (14) **RTGNN** [WWW23] (29), (15) **CLNode** [WSDM23] (38). Detailed descriptions of all the baselines can be found in Appendix C.2.

Parameter Configuration. The number of the SVD parameter m in Equation (4) is set 10, and the number of smoothing factor α in Equation (8) is set 0.85. The number of the contribution score β in Equation (11) is set 1. The detailed ablation study on hyperparameters is placed in Sec. 4.4.

4.2 MAIN RESULTS (RQ1)

We systematically evaluated our method across a spectrum of noise environments. The experiments included both uniform and pair noise types, with noise ratios set at 0.2, 0.5 and 0.7 to simulate varying levels of label corruption. The performance results are presented in Tab. 1, demonstrating consistent superiority of our approach. We summarize the key observations as follows:

Takeaway ①: AURA demonstrates consistent robustness under diverse noise conditions. As evidenced by Tab. 1, our method demonstrates remarkable robustness under 50% moderate-noise environments, consistently outperforming state-of-the-art FL and FGL baselines across both uniform and pair noise patterns on diverse datasets. A notable example is the Coauthor-CS dataset with GCN backbone under 50%-uniform noise, where AURA achieves an accuracy of 22.31%—surpassing the best baseline, CRGNN (11.09%), by a significant margin of 11.22 percentage points. This substantial performance gap underscores the effectiveness of our noise mitigation strategy.

The superiority of AURA extends beyond moderate-noise scenarios, as shown in Figure 3a, where it maintains an average performance gain ranging from 4.07% to 19.01% across both high-noise and low-noise environments compared to all baselines. More experimental results can be found in ??.

Moreover, AURA demonstrates stable and superior performance across varying client scales, highlighting its robust scalability. As illustrated in Figure 3b, our framework achieves significantly better performance than other methods in scenarios with both 10 and 15 clients.

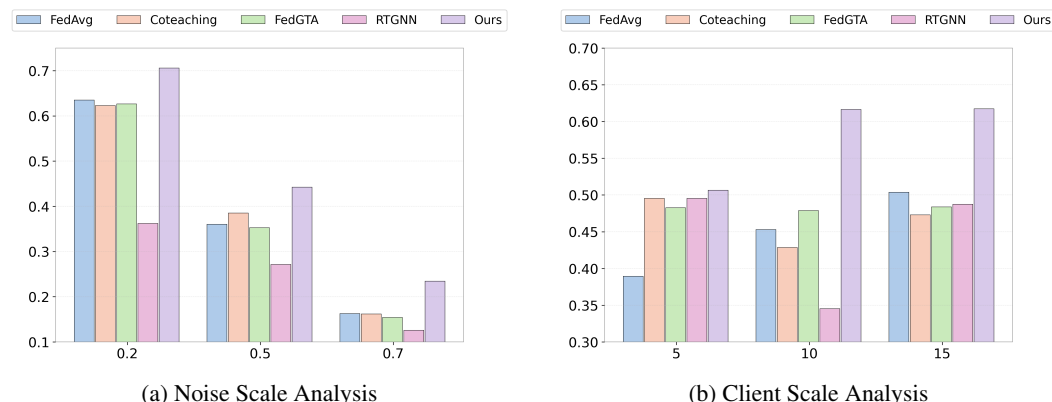


Figure 3: Performance comparison under varying scales: (a) noise rate scaling; (b) number of clients scaling. Purple bars indicate the performance of AURA. Experiments conducted on Cora and Citeseer datasets with 50% uniform noise. Our method demonstrates consistent superiority across both scaling scenarios, exhibiting remarkable robustness to increasing noise levels and stable performance with growing client populations.

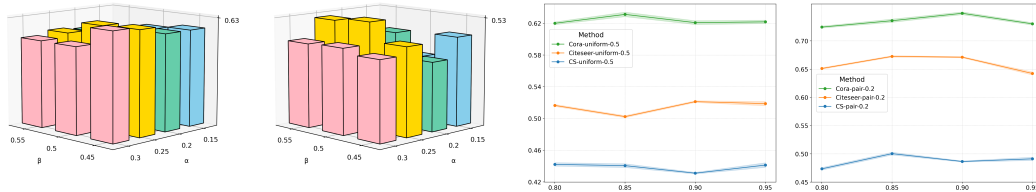
Takeaway ②: AURA achieves state-of-the-art performance in clean settings. More importantly, Tab. 1 reveals that AURA not only excels in challenging noisy conditions but also achieves state-of-the-art performance in clean settings, demonstrating its versatility and general applicability across various data quality scenarios. The consistent excellence across this spectrum of conditions highlights the methodological robustness of our approach.

432 4.3 ABLATION STUDY (RQ2)
433

434 We conduct an ablation study on the key components of **AURA** both at the client-side and server-side.
 435 Tab. 2 reports the performance of **AURA** and its variants by removing specific components from SFA
 436 to SCD. We observe that both components significantly improve framework performance. Notably,
 437 **AURA** accurately decouples label noise and interference from spectral heterogeneity while ensuring
 438 excellent performance. SFA effectively filters out high-frequency variations arising from structural
 439 differences among clients, thereby mitigating client drift. Meanwhile, SCD elevates knowledge
 440 transfer from a hard alignment to a soft one, significantly enhancing generalization and stability.
 441 Importantly, when both SFA and SCD are combined, performance reaches its peak.

442 443 4.4 SENSITIVITY STUDY (RQ3)
444

445 We investigate the impact of final
 446 loss parameter α and β , on the per-
 447 formance of **AURA**. Specifically, we
 448 vary $\alpha \in \{0.15, 0.2, 0.25, 0.3\}$, and
 449 $\beta \in \{0.45, 0.5, 0.55\}$ on Cora and Cite-
 450 seer datasets. Noise setting is 50%-uniform
 451 and 50%-pair. We observe from Figure 4 (a,
 452 b) that $\alpha = 0.25$ and $\beta = 0.5$ lead to an
 453 outstanding performance. Overall, the evalua-
 454 tion metrics demonstrate minimal fluctuations
 455 across different hyperparameter choices. In
 456 most of our experiments, we set the default
 457 values as 0.5 for α and 0.25 for β . Similarly
 458 we investigate the impact of the random walk
 459 parameter on the framework's performance. We report the performance of **AURA** on the Cora,
 460 Citeseer, and CS datasets under different noise settings, as illustrated in the Figure 4 (c, d). Based
 461 on the experimental results, we ultimately set this parameter to 0.85.



462
 463
 464
 465
 466
 467
 468
 469
 470
 471
 472
 473
 474
 475
 476
 477
 478
 479
 480
 481
 482
 483
 484
 485
 Figure 4: **Hyperparameter Analysis of AURA.** (a,b) Accuracy vs. α and β on Cora and Citeseer under uniform-50% noise. (c,d) Accuracy vs. random walk parameter δ on multiple datasets: Cora (green), CS (blue), and Citeseer (yellow); (c) uniform-50% and (d) pair-20% noise.

5 CONCLUSION

476 In this work, we propose an innovative exploration of robust FGL in noisy environment. To achieve
 477 this goal, we introduce **AURA**, a novel framework that tackles this challenge from both structural
 478 and semantic perspectives. At the client level, our Structural-aware Frequency Alignment (SFA)
 479 module leverages low-rank approximation to decompose local graphs into a structural backbone
 480 and a redundant view. By enforcing consistency between these views, we effectively purify node
 481 representations from both intra-client label noise and inter-client spectral heterogeneity, mitigating
 482 client drift. Concurrently, at the server level, our Semantic-guided Consensus Distillation (SCD)
 483 method constructs a high-quality global prototype graph from consensual client knowledge. This
 484 graph serves as a semantic anchor, guiding local models through relational knowledge distillation to
 485 align their semantic understanding, which overcomes the limitations of naive aggregation. Extensive
 486 experiments on six datasets confirm the superiority of **AURA**, demonstrating significant performance
 487 gains over state-of-the-art methods under various noise conditions.

486 REFERENCES
487

488 [1] D. A. E. Acar, Y. Zhao, R. Matas, M. Mattina, P. Whatmough, and V. Saligrama. Federated
489 learning based on dynamic regularization. In *ICLR*, 2021.

490 [2] D. Baranovskiy, I. Oseledets, and A. Babenko. A critical look at the evaluation of gnns under
491 heterophily: Are we really making progress? *arXiv preprint arXiv:2302.11640*, 2023.

492 [3] K. Canese and S. Weis. Pubmed: the bibliographic database. *The NCBI handbook*, 2(1), 2013.

493 [4] J. Chen, B. Li, Q. He, and K. He. Pamt: A novel propagation-based approach via adaptive
494 similarity mask for node classification. *IEEE Transactions on Computational Social Systems*,
495 11(5):5973–5983, 2024.

496 [5] Z. Di, Z. Zhu, X. Li, and Y. Liu. Federated learning with local openset noisy labels. In
497 A. Leonardis, E. Ricci, S. Roth, O. Russakovsky, T. Sattler, and G. Varol, editors, *Computer
498 Vision – ECCV 2024*. Springer Nature Switzerland, 2025.

499 [6] J. Fang, Z. Shao, S. Choy, and J. Gao. Svdformer: Direction-aware spectral graph embedding
500 learning via svd and transformer. *arXiv preprint arXiv:2508.13435*, 2025.

501 [7] L. Gao, H. Fu, L. Li, Y. Chen, M. Xu, and C.-Z. Xu. Feddc: Federated learning with non-iid
502 data via local drift decoupling and correction. In *CVPR*, 2022.

503 [8] X. Gao, H. Yin, T. Chen, G. Ye, W. Zhang, and B. Cui. Robgc: Towards robust graph condens-
504 ation, 2025.

505 [9] C. L. Giles, K. D. Bollacker, and S. Lawrence. Citeseer: An automatic citation indexing
506 system. In *Proceedings of the third ACM conference on Digital libraries*, pages 89–98, 1998.

507 [10] B. Han, Q. Yao, X. Yu, G. Niu, M. Xu, W. Hu, I. Tsang, and M. Sugiyama. Co-teaching:
508 Robust training of deep neural networks with extremely noisy labels, 2018.

509 [11] C. He, K. Balasubramanian, E. Ceyani, C. Yang, H. Xie, L. Sun, L. He, L. Yang, P. S. Yu,
510 Y. Rong, P. Zhao, J. Huang, M. Annavararam, and S. Avestimehr. Fedgraphnn: A federated
511 learning system and benchmark for graph neural networks, 2021.

512 [12] W. Huang, G. Wan, M. Ye, and B. Du. Federated graph semantic and structural learning. 2023.

513 [13] W. Huang, M. Ye, B. Du, and X. Gao. Few-shot model agnostic federated learning. In *ACM
514 MM*, pages 7309–7316, 2022.

515 [14] W. Huang, M. Ye, Z. Shi, G. Wan, H. Li, B. Du, and Q. Yang. A federated learning for
516 generalization, robustness, fairness: A survey and benchmark. *arXiv*, 2023.

517 [15] L. Jiang, Z. Zhou, T. Leung, L.-J. Li, and L. Fei-Fei. Mentornet: Learning data-driven curricu-
518 lum for very deep neural networks on corrupted labels, 2018.

519 [16] S. P. Karimireddy, S. Kale, M. Mohri, S. J. Reddi, S. U. Stich, and A. T. Suresh. Scaffold:
520 Stochastic controlled averaging for on-device federated learning. In *ICML*, 2020.

521 [17] J. Li, R. Socher, and S. C. H. Hoi. Dividemix: Learning with noisy labels as semi-supervised
522 learning, 2020.

523 [18] T. Li, A. K. Sahu, M. Zaheer, M. Sanjabi, A. Talwalkar, and V. Smith. Federated optimization
524 in heterogeneous networks. *Proceedings of Machine Learning and Systems*, 2:429–450, 2020.

525 [19] X. Li, K. Huang, W. Yang, S. Wang, and Z. Zhang. On the convergence of fedavg on non-iid
526 data. *arXiv preprint arXiv:1907.02189*, 2019.

527 [20] X. Li, Q. Li, D. Li, H. Qian, and J. Wang. Contrastive learning of graphs under label noise.
528 *Neural Networks*, 172:106113, 2024.

529 [21] X. Li, Z. Wu, W. Zhang, Y. Zhu, R.-H. Li, and G. Wang. Fedgta: Topology-aware averaging
530 for federated graph learning. *Proc. VLDB Endow.*, 17(1):41–50, Sept. 2023.

540 [22] R. Liu and H. Yu. Federated graph neural networks: Overview, techniques and challenges.
541 *arXiv preprint arXiv:2202.07256*, 2022.

542 [23] Y. Lu, L. Chen, Y. Zhang, Y. Zhang, B. Han, Y. ming Cheung, and H. Wang. Federated learning
543 with extremely noisy clients via negative distillation, 2024.

545 [24] E. Malach and S. Shalev-Shwartz. Decoupling "when to update" from "how to update". In
546 *Proceedings of the 31st International Conference on Neural Information Processing Systems*,
547 NIPS'17, page 961–971, Red Hook, NY, USA, 2017. Curran Associates Inc.

548 [25] A. K. McCallum, K. Nigam, J. Rennie, and K. Seymore. Automating the construction of
549 internet portals with machine learning. *Information Retrieval*, 3:127–163, 2000.

551 [26] B. McMahan, E. Moore, D. Ramage, S. Hampson, and B. A. y Arcas. Communication-efficient
552 learning of deep networks from decentralized data. In *Artificial intelligence and statistics*,
553 pages 1273–1282. PMLR, 2017.

555 [27] S. Mehta and A. Aneja. Securing data privacy in machine learning: The fedavg of federated
556 learning approach. In *2024 4th Asian Conference on Innovation in Technology (ASIANCON)*,
557 pages 1–5. IEEE, 2024.

558 [28] G. Patrini, A. Rozza, A. Menon, R. Nock, and L. Qu. Making deep neural networks robust to
559 label noise: a loss correction approach, 2017.

560 [29] S. Qian, H. Ying, R. Hu, J. Zhou, J. Chen, D. Z. Chen, and J. Wu. Robust training of graph
561 neural networks via noise governance. In *WSDM*, 2023.

563 [30] S. Reed, H. Lee, D. Anguelov, C. Szegedy, D. Erhan, and A. Rabinovich. Training deep neural
564 networks on noisy labels with bootstrapping, 2015.

566 [31] O. Shchur, M. Mumme, A. Bojchevski, and S. Günnemann. Pitfalls of graph neural network
567 evaluation. *arXiv preprint arXiv:1811.05868*, 2018.

568 [32] O. Shchur, M. Mumme, A. Bojchevski, and S. Günnemann. Pitfalls of graph neural network
569 evaluation. In *NeurIPS Workshop*, 2018.

571 [33] P. Shirzadian, B. Antony, A. G. Gattani, N. Tasnina, and L. S. Heath. A time evolving online
572 social network generation algorithm. 13(1):2395.

573 [34] H. Song, M. Kim, D. Park, Y. Shin, and J.-G. Lee. Learning from noisy labels with deep
574 neural networks: A survey. *IEEE Transactions on Neural Networks and Learning Systems*,
575 34(11):8135–8153, 2023.

577 [35] V. Tsouvalas, A. Saeed, T. Ozcelebi, and N. Meratnia. Labeling chaos to learning harmony:
578 Federated learning with noisy labels. *ACM Trans. Intell. Syst. Technol.*, 2024.

579 [36] G. Wan, Z. Shi, W. Huang, G. Zhang, D. Tao, and M. Ye. Energy-based backdoor defense
580 against federated graph learning. In *International Conference on Learning Representations*,
581 2025.

583 [37] G. Wan, Y. Tian, W. Huang, N. V. Chawla, and M. Ye. S3gcl: Spectral, swift, spatial graph
584 contrastive learning. In *Forty-first International Conference on Machine Learning*, 2024.

585 [38] X. Wei, X. Gong, Y. Zhan, B. Du, Y. Luo, and W. Hu. Clnode: Curriculum learning for node
586 classification. In *Proceedings of the Sixteenth ACM International Conference on Web Search*
587 and Data Mining, WSDM '23, page 670–678, New York, NY, USA, 2023. Association for
588 Computing Machinery.

590 [39] N. Wu, L. Yu, X. Jiang, K.-T. Cheng, and Z. Yan. Fednoro: Towards noise-robust federated
591 learning by addressing class imbalance and label noise heterogeneity, 2023.

592 [40] J. Xu, Z. Chen, T. Q. Quek, and K. F. E. Chong. Fedcorr: Multi-stage federated learning for
593 label noise correction. In *CVPR*, pages 10184–10193, 2022.

594 [41] X. Yu, B. Han, J. Yao, G. Niu, I. Tsang, and M. Sugiyama. How does disagreement help
595 generalization against label corruption? In *Proceedings of the 36th International Conference*
596 *on Machine Learning*, pages 7164–7173. PMLR, 2019.

597 [42] X. Yu, B. Han, J. Yao, G. Niu, I. W. Tsang, and M. Sugiyama. How does disagreement help
598 generalization against label corruption?, 2019.

600 [43] C. Zhang, S. Bengio, M. Hardt, B. Recht, and O. Vinyals. Understanding deep learning requires
601 rethinking generalization, 2017.

602 [44] Q. Zhang, Z. Ma, P. Zhang, and E. Jenelius. Mobility knowledge graph: Review and its
603 application in public transport.

605 [45] X.-M. Zhang, L. Liang, L. Liu, and M.-J. Tang. Graph neural networks and their current
606 applications in bioinformatics. 12.

608 [46] Y. Zhu, X. Li, M. Hu, and D. Wu. Federated continual graph learning. *arXiv preprint*
609 *arXiv:2411.18919*, 2024.

610 [47] Y. Zhu, X. Li, Z. Wu, D. Wu, M. Hu, and R.-H. Li. Fedtad: Topology-aware data-free knowl-
611 edge distillation for subgraph federated learning. *arXiv preprint arXiv:2404.14061*, 2024.

612
613
614
615
616
617
618
619
620
621
622
623
624
625
626
627
628
629
630
631
632
633
634
635
636
637
638
639
640
641
642
643
644
645
646
647

648
649
A NOTATIONS650
651
652
653
654
655
656
657
658
659
660
661
662
663
664
665
666
667
668
669
670
671
672
673
674
675
676
677
678
679
680
681
682
683
684
685
686
687
688
689
690
691
692
693
694
695
696
697
698
699
700
701
We present a comprehensive review of the commonly used notations and their definitions in Tab. 3.652
653
Table 3: Notations and Definitions.

Notation	Definition
$\mathcal{G}_k = \{\mathcal{V}_k, \mathcal{A}_k, \mathcal{X}_k\}$	Input data for the m -th client
\mathcal{A}_k	The adjacency matrix of \mathcal{G}_k
\mathcal{X}_k	The feature matrix of \mathcal{G}_k
\mathcal{Y}_k	The one-hot label matrix of \mathcal{G}_k
h_k	The embeddings from the original graph \mathcal{G}_k
K	The number of clients
d	The dimension of the node feature
ϵ	The fixed probability that the true label is flipped to a specific paired class
$\sum_k^{[1:m]}$	The top- m diagonal structural pattern for the m -th client
$\hat{\mathbf{A}}_k$	The loss-pass filtered representation of the original graph structure
C_{ij}	The cost of matching node v_i from the original view to node v_j from the backbone view
P_{ij}	The transport plan that minimizes the total transportation cost
$\langle \cdot, \cdot \rangle_F$	The Frobenius dot product
$\Pi(\mathbf{r}, \mathbf{c})$	The set of joint probability matrices with uniform marginals \mathbf{r} and \mathbf{c}
D	The degree matrix
I	The identity matrix
M	The global influence matrix
α	The smoothing factor
$Score_i^b$	The Breadth influence for node i
$Score_i^d$	The Depth influence for node i
τ_i	The optional weight or type coefficient for node i
β	The hyperparameter used to adjust the weight of Depth Influence
\mathbf{p}_k^c	The local prototype of class c for client k
S_i^c	The similarity score of prototypes i from class c

685
686
B RELATED WORK.687
688
689
690
691
692
693
694
695
696
697
698
699
700
701
Federated Graph Learning(FGL). Federated Graph Learning (FGL) extends Federated Learning (FL) to graph-structured data, enabling decentralized training while preventing the exposure of raw graph data, thus enhancing privacy protection (11; 14; 22; 4; 37; 36). Despite extensive research dedicated to enhancing model performance, the presence of noise in datasets, such as erroneous node labels, poses a significant threat to a model’s generalization capabilities. To overcome this limitation, we propose a robust Federated Graph Learning (FGL) framework based on hyperspherical representation learning. This framework enhances the model’s ability to extract the principal update direction from clients, thereby maintaining stable classification performance in scenarios characterized by both label noise and data heterogeneity.696
Robust Federated Learning and Graph Learning.697
698
699
700
701
The presence of noisy labels in Federated Learning, particularly when applied to graph-structured data, presents a core challenge to model robustness and generalization. Existing solutions to this problem predominantly follow two main paradigms: label correction and self-supervised learning. Label correction methods aim to directly identify and rectify erroneous annotations. Such techniques typically rely on representations learned from training data, for instance, by reassigning noisy labels based on nearest-neighbor relationships (35) in the embedding space or through predictions from a

global model(5). Although established techniques like loss correction (30; 28) and sample selection (10; 15; 17; 24; 42) exist for learning with noisy labels in traditional graph learning, they are not directly applicable to training GNNs in a federated setting, especially under conditions of limited label noise and data heterogeneity. A critical bottleneck is that most existing approaches implicitly assume a homogeneous data distribution, causing their performance to degrade in real-world non-IID scenarios. This often results in the intermixture of effective signals and noise components within the feature space. Pivoting from these limitations, our research is the first to systematically apply the self-supervised learning paradigm to construct a robust federated graph learning framework. We aim to leverage the intrinsic structure of the data itself to overcome the dual challenges posed by label noise and data heterogeneity.

C EXPERIMENTAL DETAILS.

C.1 DATASET DETAILS

To assess the effectiveness of **AURA**, we conduct experiments on five real-world graph datasets: Cora, CiteSeer, PubMed, Physics, and CS. Each dataset is split into training, validation, and test sets in a fixed 20%/40%/40% ratio. The key statistics of these datasets are summarized in Tab. 4. A detailed description is provided below:

- **Cora, CiteSeer, and PubMed.** These three citation network datasets are standard benchmarks in graph-based machine learning, especially for tasks like node classification and link prediction. In these datasets, nodes correspond to academic papers, while edges represent citation links. Each node is assigned a class label, and its feature vector is constructed from textual information such as words in the title or abstract. These datasets exhibit sparsity and high dimensionality, making them well-suited for evaluating the effectiveness and scalability of graph neural networks (GNNs).
- **Coauthor-Physics.** Coauthor-Physics is an academic network containing co-authorship relationships based on the Microsoft Academic Graph. Nodes in the graph represent authors and edges represent co-authorship relationships. In the dataset, authors are categorized into five classes based on their research areas, and the nodes are characterized as bag-of-words representations of keywords of papers.
- **Coauthor-CS.** Coauthor-CS represents a co-authorship network in the field of computer science, where nodes correspond to research papers, and edges denote co-authorship relations. Each paper is associated with a topic category, and features are extracted from the paper’s title and abstract. This dataset is commonly used to evaluate node classification and community detection algorithms.

Dataset	#Nodes	#Edges	#Classes	#Features
Cora	2,708	5,278	7	1,433
CiteSeer	3,327	4,552	6	3,703
Pubmed	19,717	44,324	3	500
Coauthor-Physics	34,493	530,417	5	8,415
Coauthor-CS	18,333	327,576	15	6,805

Table 4: **Statistics** of datasets used in experiments.

C.2 COUNTERPART DETAILS

This section provides a comprehensive overview of the baseline approaches employed in our study.

- **FedAvg** [ASTAT17]. A foundational algorithm in Federated Learning, FedAvg operates by allowing clients to independently train models on their local datasets and subsequently transmit their model updates to a central server. The server performs a weighted aggregation of these updates to refine the global model, which is then redistributed to the clients for further local training. By transmitting only model parameters instead of raw data, FedAvg reduces communication costs and enhances privacy. However, it struggles with performance degradation in scenarios where client data distributions are highly non-IID (19; 27).

- **FedProx** [MLSys20]. As an enhancement of FedAvg, FedProx is specifically designed to address the challenges posed by statistical heterogeneity in federated learning. It introduces an additional regularization term that constrains local updates, preventing excessive divergence from the global model. This proximal term mitigates the impact of local data distribution shifts, leading to more stable convergence. By ensuring consistency in updates across clients, FedProx demonstrates improved robustness in non-IID settings.
- **FedDC** [NeurIPS20]. FedDC addresses local model drift caused by non-independent and identically distributed (Non-IID) data across clients. It introduces a local drift decoupling and correction mechanism, where an auxiliary variable on each client tracks the gap between local model updates and the global model. This approach enforces consistency at the parameter level, leading to accelerated convergence and strong performance in heterogeneous environments with partial client participation.
- **FedDyn** [ICLR21]. FedDyn addresses the inconsistency between local client objectives and the global optimization goal. It introduces a dynamic regularization method that modifies each client's objective function every round, aligning the stationary points of the local objectives with that of the global objective. This ensures that even with heterogeneous data, the local updates correctly contribute to the global goal, achieving robust performance in both convex and non-convex settings with imbalanced data and device heterogeneity.
- **Scaffold** [ICML20]. Scaffold addresses the "client drift" problem in federated learning caused by heterogeneous data distributions across clients. It corrects for this drift by using control variates to estimate the update direction of the global model and the drift of each local model. This variance reduction technique modifies local updates to better align with the global objective, ensuring faster and more stable convergence while achieving higher accuracy in Non-IID settings.
- **FedGTA** [VLDB24]. FedGTA is tailored for large-scale graph federated learning, tackling issues of slow convergence and suboptimal scalability. Unlike prior methods that focus on either optimization strategies or complex local models, FedGTA integrates topology-aware local smoothing with mixed neighbor feature aggregation to improve learning efficiency (46). By leveraging graph structures in aggregation, it enhances scalability and performance in federated graph learning.
- **FedTAD** [IJCAI24]. FedTAD addresses subgraph heterogeneity in FL by decomposing local graph variations into label and structural differences, preventing inconsistent model aggregation. It enhances knowledge transfer via topology-aware distillation, boosting FL reliability and efficiency.
- **FGSSL** [IJCAI23]. FGSSL addresses local client distortion caused by both node-level semantics and graph-level structures. It improves discrimination by contrasting nodes from different classes, aligning local nodes with their global counterparts of the same class while pushing them away from different classes. To handle structural information, it transforms adjacency relationships into similarity distributions and distills relational knowledge from the global model into local models. This approach preserves both structural integrity and discriminability, achieving superior performance on multiple graph datasets.
- **Coteaching** [NeurIPS18]. Coteaching addresses the challenge of training deep learning models with noisy labels that can degrade performance. It proposes a dual-network approach where two models are trained simultaneously. In each mini-batch of data, each network selects samples with the smallest training loss—which are likely to be correctly labeled—and teaches these samples to its peer network for the subsequent parameter update. This collaborative process prevents the models from overfitting to mislabeled data, significantly improving their robustness and generalization on datasets with noisy labels.
- **FedNoRo** [IJCAI23]. FedNoRo adopts a two-stage framework to address class-imbalanced global data with heterogeneous label noise in federated learning. The method first identifies noisy clients through per-class loss indicators and Gaussian Mixture Modeling, then performs noise-robust federated updates via joint knowledge distillation and distance-aware aggregation, specifically designed for realistic medical scenarios with data imbalance and complex noise patterns.
- **FedNed** [AAAI24]. FedNed adopts a negative distillation framework to effectively leverage extremely noisy clients in federated learning. The method first identifies noisy clients, then innovatively utilizes them as 'bad teachers' through a dual-training approach: one model trained on original noisy labels for reverse knowledge distillation, and another on global model-generated pseudo-labels for conditional participation in aggregation. This approach transforms noisy clients from detrimental elements into valuable contributors while progressively enhancing their trustworthiness through pseudo-label refinement

810 • **FedCorr** [CVPR22]. FedCorr adopts a multi-stage framework to address heterogeneous label
 811 noise in federated learning while preserving data privacy. The method first dynamically identifies
 812 noisy clients through model prediction subspace analysis and per-sample loss evaluation, then
 813 employs an adaptive local proximal regularization to handle data heterogeneity. After fine-tuning
 814 on clean clients and correcting labels for noisy ones, FedCorr performs final training across all
 815 clients to fully utilize available data, effectively handling varying noise levels without requiring
 816 prior assumptions about client noise models.

817 • **CRGNN** [NN24]. CRGNN addresses label noise in GNNs by combining neighborhood-based la-
 818 bel correction and contrastive learning. It utilizes message passing neural networks to update node
 819 representations, integrating graph contrastive learning for consistent representations across aug-
 820 mented graph views. Finally, CGNN employs an MLP for prediction distributions and iteratively
 821 corrects noisy labels by comparing them with their neighbors and choosing the most labels.

822 • **RTGNN** [WWW23]. RTGNN proposes a noise governance framework that combines self-
 823 reinforcement supervision for noisy label correction and consistency regularization to prevent
 824 overfitting. The method categorizes labels into clean and noisy types, then applies adaptive super-
 825 vision by rectifying inaccurate labels and generating pseudo-labels for unlabeled nodes, enabling
 826 effective learning from clean labels while mitigating noise impact.

827 • **CLNode** [WSDM23]. CLNode addresses the difficulty of training Graph Neural Networks
 828 (GNNs) on complex graphs for node classification tasks. It introduces a curriculum learning strat-
 829 egy that organizes training samples in a meaningful order, from easy to difficult, based on node
 830 characteristics. By allowing the model to first learn from simpler nodes and gradually progress to
 831 more complex ones, it helps the model better capture intricate structural patterns and relationships.
 832 This approach enhances the overall training process and leads to superior performance on various
 833 node classification benchmarks.

D ALGORITHM WORKFLOW

The AURA algorithm framework is presented in Algorithm 1.

Algorithm 1 AURA Framework

Input: Communication rounds T , participant scale K , k -th client private model θ_k , k -th client local data \mathcal{G}_k and loss weight β
Output: The final global model θ_{global}

for $t = 1, 2, \dots, T$ **do**

Client Side: for $m = 1$ **to** K **in parallel do**

$\hat{\mathbf{A}}_k \leftarrow \text{SVDandReconstruct}(\mathcal{G}_k, \mathcal{A}_k)$ **by** Equation (4) *// Decompose original graph and re-*
construct low-frequency adjacency matrix

$\mathcal{L}_{SFA} \leftarrow \text{Sinkhorn}(\mathbf{H}_k, \hat{\mathbf{H}}_k)$ **by** Equation (6) *// Graph Spectral Structural Alignment*

$Score_i^b \leftarrow \text{BreadthInfluence}(\mathcal{G}_k)$ **by** Equation (9) *// Calculate Breadth Influence for each*
node

$Score_i^d \leftarrow \text{DepthInfluence}(\mathcal{G}_k)$ **by** Equation (10) *// Calculate Depth Influence for each node*

$\mathbf{P} \leftarrow \text{CalculatePrototypes}(Score_i^b, Score_i^d, \mathcal{G}_k)$ **by** Equation (12) *// Select node and calcu-*
late prototypes

$\mathcal{L}_{FKD} \leftarrow \text{LocalKnowledgeAlignment}(\mathbf{P}_g, \mathbf{h}^g, \mathbf{h}^i)$ **by** Equation (15) *// Semantic-guided*
Consensus Distillation

$\theta_m^{t+1} \leftarrow \text{LocalUpdating}(\theta_m^t, \mathcal{L}_{SFA} + \beta \mathcal{L}_{FKD})$ *// Backward propagation*

Server Side:

$\mathcal{M}_{sim}^c = \text{CalculateSimilarity}(\mathbf{p}^c), \forall c$ **by** Equation (13) *// Calculate prototypes similarity*

$\mathbf{P}_g^c \leftarrow \text{SelectPrototypes}(\mathcal{M}_{sim}^c), \forall c$ **by** Equation (14) *// Select Prototypes by similarity matrix*

$\theta_{global} \leftarrow \text{Aggregate}(\theta_k), \forall k$ *// Clean clients aggregation*

$\theta_k \leftarrow \theta_{global}, \forall k$ *// Distribute parameters to clients*

return θ_{global}

Table 5: Performance comparison to state-of-the-art methods when poisoning 20% of the full set.

864	865	Dataset	CORA (Acc \uparrow)			CITESEET (Acc \uparrow)			PUBMED (Acc \uparrow)		
			Noise Type	Normal	Uniform	Pair	Normal	Uniform	Pair	Normal	Uniform
866	867	FedAvg [ASTAT17]	74.50 \pm 0.00	68.83 \pm 0.00	67.55 \pm 0.00	64.15 \pm 0.00	43.70 \pm 0.00	52.44 \pm 0.00	84.16 \pm 0.00	84.36 \pm 0.00	83.07 \pm 0.00
		FedProx [MLSys20]	75.32 \pm 0.82	68.92 \pm 0.00	69.56 \pm 0.21	65.19 \pm 0.04	45.33 \pm 0.63	51.26 \pm 0.18	84.24 \pm 0.08	84.46 \pm 0.10	83.25 \pm 0.18
		FedDC [CVPR22]	80.90 \pm 0.40	67.55 \pm 0.28	70.02 \pm 0.47	67.85 \pm 0.70	53.04 \pm 0.34	57.33 \pm 0.89	82.91 \pm 0.35	53.04 \pm 31.32	44.81 \pm 38.26
		FedDyn [ICLR21]	79.98 \pm 0.48	67.82 \pm 0.01	69.20 \pm 0.15	69.04 \pm 0.89	52.89 \pm 0.19	56.59 \pm 0.15	81.83 \pm 0.23	81.10 \pm 0.97	75.81 \pm 0.76
		Scaffold [ICML20]	81.90 \pm 0.70	73.40 \pm 0.57	71.85 \pm 0.30	70.22 \pm 0.07	56.96 \pm 13.26	62.07 \pm 0.63	75.25 \pm 0.59	72.77 \pm 11.59	65.54 \pm 17.53
		FedGTA [VLDB24]	72.21 \pm 0.29	71.57 \pm 0.74	68.46 \pm 0.91	65.33 \pm 0.18	48.74 \pm 0.04	56.59 \pm 0.15	82.41 \pm 01.75	83.35 \pm 0.01	81.83 \pm 0.24
		FedTAD [IJCAI24]	64.90 \pm 0.60	62.61 \pm 0.22	63.35 \pm 0.20	64.30 \pm 0.18	44.44 \pm 0.74	52.59 \pm 0.15	84.36 \pm 0.20	84.59 \pm 0.23	82.97 \pm 0.10
873	872	FGSSL [IJCAI23]	68.74 \pm 0.16	69.20 \pm 0.37	66.27 \pm 0.28	70.07 \pm 0.92	64.30 \pm 20.60	62.81 \pm 10.37	67.03 \pm 17.13	72.34 \pm 12.02	66.57 \pm 16.50
		Coteaching [NeurIPS18]	72.03 \pm 0.47	67.37 \pm 0.46	66.82 \pm 0.73	64.30 \pm 0.15	54.22 \pm 10.52	56.74 \pm 0.40	84.26 \pm 0.10	82.52 \pm 0.84	83.40 \pm 0.33
		FedNoRo [IJCAI23]	74.50 \pm 0.00	68.83 \pm 0.00	67.37 \pm 0.18	67.76 \pm 0.61	43.70 \pm 0.00	52.44 \pm 0.00	84.16 \pm 0.00	84.36 \pm 0.00	83.07 \pm 0.00
		FedNed [AAAI24]	69.84 \pm 0.66	56.58 \pm 12.25	55.94 \pm 11.61	57.78 \pm 0.37	37.33 \pm 0.37	46.07 \pm 0.37	84.56 \pm 0.40	81.63 \pm 02.73	79.91 \pm 03.16
		FedCorr [CVPR22]	75.14 \pm 0.64	67.82 \pm 0.01	65.63 \pm 0.92	38.96 \pm 25.19	30.07 \pm 13.63	34.07 \pm 18.87	85.93 \pm 01.77	84.69 \pm 00.33	84.64 \pm 01.57
		CRGNN [NN24]	72.30 \pm 0.20	67.28 \pm 0.55	67.92 \pm 0.37	69.33 \pm 05.18	60.00 \pm 16.30	62.37 \pm 09.93	84.08 \pm 0.08	83.40 \pm 0.96	83.38 \pm 0.31
		RTGNN [WWW23]	71.46 \pm 03.04	59.60 \pm 09.23	54.57 \pm 12.98	67.85 \pm 03.70	60.33 \pm 16.63	66.67 \pm 14.23	60.10 \pm 24.06	74.49 \pm 09.87	65.71 \pm 17.36
877	876	CLNode [WSDM23]	69.65 \pm 04.85	57.68 \pm 11.15	57.59 \pm 09.96	59.11 \pm 05.04	40.59 \pm 03.11	48.74 \pm 03.70	84.99 \pm 00.83	82.06 \pm 02.30	80.74 \pm 02.33
		AURA	85.22 \pm 10.72	75.50 \pm 06.67	73.58 \pm 06.03	77.23 \pm 13.08	65.56 \pm 21.86	67.26 \pm 14.82	85.95 \pm 01.79	86.15 \pm 01.79	82.11 \pm 00.96
		Whole Dataset	62.13 \pm 0.9			49.12 \pm 0.3			80.54 \pm 0.0		
		Dataset	COAUTHOR-PHYSICS (F1-macro \uparrow)			MINESWEEPER (F1-macro \uparrow)			COAUTHOR-CS (F1-macro \uparrow)		
		Noise Type	Normal	Uniform	Pair	Normal	Uniform	Pair	Normal	Uniform	Pair
		FedAvg [ASTAT17]	24.18 \pm 0.00	15.58 \pm 00.00	37.93 \pm 00.00	53.51 \pm 00.00	50.16 \pm 00.00	47.22 \pm 00.00	02.47 \pm 00.00	02.47 \pm 00.00	02.47 \pm 00.00
		FedProx [MLSys20]	23.22 \pm 00.96	19.81 \pm 04.23	46.06 \pm 08.13	53.54 \pm 00.03	51.25 \pm 01.09	47.42 \pm 00.20	02.76 \pm 00.29	02.72 \pm 00.25	03.12 \pm 00.65
881	880	FedDC [CVPR22]	13.55 \pm 10.63	13.46 \pm 02.12	13.46 \pm 24.47	53.59 \pm 00.08	46.52 \pm 03.64	44.33 \pm 02.89	03.22 \pm 00.75	03.09 \pm 00.62	02.54 \pm 00.07
		FedDyn [ICLR21]	15.78 \pm 08.40	13.61 \pm 01.97	21.69 \pm 16.24	51.22 \pm 02.29	50.23 \pm 00.07	44.33 \pm 02.89	06.38 \pm 03.91	06.05 \pm 03.58	04.09 \pm 01.62
		Scaffold [ICML20]	42.61 \pm 18.43	15.21 \pm 00.37	24.66 \pm 13.27	44.25 \pm 00.26	46.45 \pm 03.71	45.01 \pm 02.21	02.46 \pm 00.01	02.47 \pm 00.00	02.47 \pm 00.00
		FedGTA [VLDB24]	13.72 \pm 10.46	13.59 \pm 01.99	32.84 \pm 05.09	53.58 \pm 00.07	51.40 \pm 01.24	46.13 \pm 01.09	01.35 \pm 01.12	03.11 \pm 00.64	03.54 \pm 01.07
		FedTAD [IJCAI24]	22.13 \pm 02.05	13.46 \pm 02.12	13.75 \pm 24.18	54.11 \pm 00.60	51.85 \pm 01.69	45.55 \pm 01.67	02.47 \pm 00.00	02.78 \pm 00.31	02.47 \pm 00.00
		FGSSL [IJCAI23]	28.13 \pm 03.95	13.46 \pm 02.12	34.25 \pm 03.68	44.46 \pm 00.05	41.98 \pm 08.18	44.33 \pm 02.89	02.83 \pm 00.36	02.47 \pm 00.00	02.14 \pm 00.33
		Coteaching [NeurIPS18]	13.46 \pm 10.72	32.29 \pm 16.71	42.52 \pm 04.59	44.25 \pm 00.26	44.78 \pm 05.38	44.33 \pm 02.89	08.00 \pm 05.53	07.37 \pm 04.90	08.22 \pm 05.75
886	885	FedNoRo [IJCAI23]	22.46 \pm 01.72	15.58 \pm 00.00	37.93 \pm 00.00	53.54 \pm 00.03	51.25 \pm 01.09	47.42 \pm 00.20	02.49 \pm 00.02	02.42 \pm 00.05	02.49 \pm 00.02
		FedNed [AAAI24]	35.94 \pm 11.76	41.90 \pm 26.32	38.51 \pm 00.58	51.97 \pm 01.54	51.94 \pm 01.78	48.79 \pm 01.57	11.85 \pm 09.38	11.57 \pm 09.10	06.75 \pm 04.28
		FedCorr [CVPR22]	27.93 \pm 03.75	28.45 \pm 15.87	34.12 \pm 03.81	44.14 \pm 01.37	41.12 \pm 09.04	44.12 \pm 03.10	01.34 \pm 01.13	08.06 \pm 05.59	02.96 \pm 00.49
		CRGNN [NN24]	35.12 \pm 10.94	47.44 \pm 31.86	44.14 \pm 06.21	46.78 \pm 06.73	43.12 \pm 07.04	44.33 \pm 02.89	13.08 \pm 10.61	11.39 \pm 08.92	11.70 \pm 09.23
		RTGNN [WWW23]	33.17 \pm 08.99	13.46 \pm 02.12	40.28 \pm 02.35	43.93 \pm 09.58	44.25 \pm 05.91	44.31 \pm 02.91	02.47 \pm 00.00	09.78 \pm 07.31	02.47 \pm 00.00
		CLNode [WSDM23]	40.78 \pm 16.60	37.96 \pm 22.38	28.14 \pm 09.79	53.93 \pm 04.42	52.41 \pm 02.25	48.30 \pm 01.08	06.83 \pm 04.36	06.83 \pm 04.36	06.81 \pm 04.34
		AURA	57.99 \pm 33.81	66.64 \pm 51.06	56.53 \pm 18.60	55.29 \pm 01.78	54.34 \pm 04.18	54.34 \pm 07.12	21.80 \pm 19.33	21.56 \pm 19.84	20.17 \pm 17.70
891	890	Whole Dataset	25.45 \pm 0.9			42.46 \pm 0.3			07.46 \pm 0.0		

E ETHICS AND SOCIETAL IMPACT

This work aims to advance the robustness of FGL by addressing challenges such as label noise and data heterogeneity. While the research primarily focuses on improving model performance and generalization in decentralized environments, we acknowledge the broader implications of deploying such models in real-world settings. One key ethical concern lies in the use of sensitive data in FL environments. Although FL inherently protects privacy by keeping data local, the potential for adversarial manipulation of models or the inadvertent leakage of sensitive information remains a risk. In this study, we do not introduce any new sensitive datasets or personal data into the models, and we adhere to the principles of privacy-preserving machine learning.

F THE USE OF LARGE LANGUAGE MODEL (LLMs)

Our use of Large Language Models (LLMs) was strictly limited to polishing the language an- search and intellectual content of this papegenerating figures for the manuscript. All underlying reincluding the AURA frawork, its theoretical foundations, experimental design, and thanalysis of results, was completed entirely by the authors without assistance from LLMs.

G ADDITIONAL EXPERIMENTAL RESULTS

We place additional Acc and F1-macro score results under 0.2 noisy label ratios in Tab. 5.